Thomas J. Urbanik[1]

Machine Direction Strength Theory of Corrugated Fiberboard

REFERENCE: Urbanik.T.J.,"Machine Direction Strength Theory of Corrugated Fiberboard," *Journal of Composites Technology & Research,* JCTRER, Vol. 18, No. 2, April 1996. pp. *80-88.*

ABSTRACT: Linerboard elements between the corrugations of corrugated fiberboard can be viewed as short wide columns when the fiberboard is loaded perpendicular to the axes of the corrugations. Column ends are elastically restrained by the corrugated medium. A theory of buckling of nonlinear corrugated fiberboard material, with compression perpendicular to the corrugation axes, was developed. This theory is consistent with a previous theory applied to fiberboard wish compression parallel to the corrugations. The theory matched strength data of corrugated fiberboard using paper compression strength, extensional stiffness, and bending stiffness data as inputs. The theory was further improved by empirically correcting for interactions between material crush failure and structure buckling failure. The correction equation predicts an optimum form of the linerboard stress-strain curve from initial slope and maximum stress data and predicts an element slenderness that varies with the mode of failure.

KEYWORDS: plate structure, elastic stability, buckling, fiberboard, paper

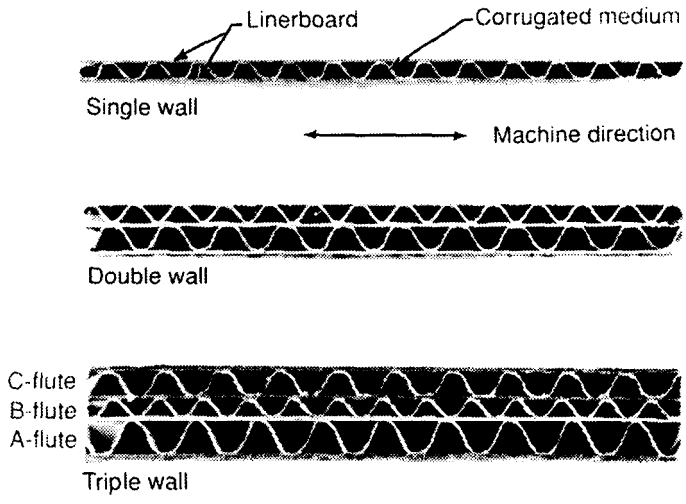

FIG. 1—Cross sections of the three constructions of corrugated fiberboard showing corrugations produced with axes perpendicular to the MD of linerboard and corrugated medium material (M134 373).

The fabrication of corrugated fiberboard yields a sandwich structure in which a linerboard material is glued to a corrugated medium. The direction of rnachining (MD) coincides with the fiber alignment of the paper and is perpendicular to the principal axes of the corrugations (Fig. 1). The direction parallel to the corrugation axes is called the cross-machine direction (CD). Standard corrugating geometries, A, B, C flute (Fig. 1), have traditionally been employed, although it is beeoming increasingly popular to produce optimum geometries with respect to paper properties. Corrugated fiberboard boxes are normally stacked in the top-to-bottom orientation where fiberboard compression strength in the CD parallel to the corrugations relates to box strength. To facilitate the tilling and dispensing of interior packages, boxes are sometimes stacked side-to-side or end-to-end or handled as unit loads by clamp trucks where MD strength becomes equally important.

Performance-based changes made to shipping regulations for corrugated boxes have motivated linerboard producers to maximize both CD paperboard strength and the expected edgewise crush test (ECT) strength of the combined board. Researchers at the Forest Products Laboratory applied buckling theory to CD paperboard *[1]* and to CD corrugated fiberboard *[2]* and predicted the importance of both MD and CD stress-strain properties. Subsequently, French researchers *[3]* experimentally corroborated the importance of MD paper strength and advocated maximizing the geometric mean of MD and CD paper strengths to maximize box strength.

When optimizing paper properties to maximize top-to-bottom box strength, the user should consider the end-use loading conditions of the box and insure that MD fiberboard strength does not suffer. The use of linerboard marketed as a "high strength" material and the greater options for customizing the corrugating geometry make this issue particularly relevant. Also, in considering MD ECT strength, the interaction between linerboard and corrugated medium becomes more critical.

Buckling theory can be used to prove that linerboard strength in CD-loaded corrugated fiberboard is a function of corrugated medium stiffness and that its strength can be increased by, at most, 1.75 times due to rigid support from the corrugating medium. With MD loading of fiberboard the linerboard becomes more unstable, but its strength can be increased up to 4 times due to rigid support from the corrugating medium. These predictions, between the extreme conditions of zero and infinite medium rigidity, quantify the importance of medium stiffness to the performance of linerboard material with CD and MD loading of corrugated fiberboard.

Objective and Scope

During paper production the compression strength of paper samples measured off-line is commonly used es a quality control

[1]Research engineer. USDA Forest Service, Forest Products Laboratory, Madison, WI 53705-2398. The Forest Products Laboratory is maintained in cooperation with the University of Wisconsin. This article was written and prepared by U.S. Government employees on official time, and it is therefore in the public domain and not subject to copyright.

1996 by the American Society for Testing and Materials

criterion. Other paper srress-strain properties that contribute to box strength might fortuitously correlate with paper strength. An understanding of how linerboard material and corrugating medium material affect box strength (according to mechanistic principles) can provide the rationale to rank various paper properties by importance and manage quality control. The objective of this paper is to broaden the buckling theory previously applied to CD-loaded corrugated fiberboard and thereby predict the strength of MD-loaded fiberboard. The global buckling of corrugated fiberboard pastels in a box is not analyzed in this report. For such an analysis, the theory developed in this paper can provide a prediction of material strength for consideration when boxes are loaded in the MD of the corrugated fiberboard.

In the treatment of the mechanics of honeycombs *[4]*, cellular walls were considered to buckle like columns with elastic ends when the honeycomb structure was compressed in a plane perpendicular to the cell axes. In the theory of corrugated fiberboard developed here, linerboard elements are considered to buckle by the same mechanism, but a nonlinear material characterization applicable to paper is added. An interaction between material crushing and buckling, found applicable to wood columns in *[5]* is used to broaden the failure mechanism and correct for apparent deviations from buckling theory.

Localized Buckling Theory

Background Terminology

Several equations and terminology from previous publications are useful in the development of equations used in this paper. In the nonlinear theory for elastic plates *[6]*, on which this paper is based, equation (2.37)[2] in the form

$$\frac{\partial^2 M_{11}}{\partial x^2} + 2\frac{\partial^2 M_{12}}{\partial x \partial y} + \frac{\partial^2 M_{22}}{\partial y^2} + \frac{\partial}{\partial x}\left(N_{11}\frac{\partial w}{\partial x} + N_{12}\frac{\partial w}{\partial y}\right) + \frac{\partial}{\partial y}\left(N_{22}\frac{\partial w}{\partial y} + N_{21}\frac{\partial w}{\partial x}\right) = 0 \qquad (1)$$

where x and y are material Cartesian coordinates, N_{ij} force resultants, M_{ij} moment resultants, and w is the transverse displacement, gives the equation of transverse force equilibrium. When applied to a component of corrugated fiberboard, the x direction is in the MD of paper; the y direction is in the CD. The moment resultants used here are derived from the moment-curvature relations given by equation (2.34) of reference *[6]* as

$$M_{11} = -\frac{1}{12}h^3\left(H_{11}\frac{\partial^2 w}{\partial x^2} + H_{12}\frac{\partial^2 w}{\partial y^2} + H_{13}\frac{\partial^2 w}{\partial x \partial y}\right)$$

$$M_{22} = -\frac{1}{12}h^3\left(H_{12}\frac{\partial^2 w}{\partial x^2} + H_{22}\frac{\partial^2 w}{\partial y^2} + H_{23}\frac{\partial^2 w}{\partial x \partial y}\right)$$

$$M_{12} = M_{21} = -\frac{1}{24}h^3\left(H_{13}\frac{\partial^2 w}{\partial x^2} + H_{23}\frac{\partial^2 w}{\partial y^2} + H_{33}\frac{\partial^2 w}{\partial x \partial y}\right) \qquad (2)$$

where h is plate thickness and H_{ij} bending stiffness moduli.

The CD edgewise crush analysis in Johnson and Urbanik [2] considered the elastic stability of a subsection of corrugated fiberboard characterized by a repeating sequence of microplates joined along the linerboard-medium attachment points. Bending stiffness moduli of each microplate were functions of respective plate curvatures in the x and y directions related to fiberboard strain in they direction. Element stiffness coefficients K_{ij} related the nodal rotation along a y- direction plate edge to the external y- direction force and varied nonlinearly with strain and bending moduli. Finite element stiffness matricies for each linerboard microplate and medium microplate were added to construct a global structure matrix for the corrugated subsection. The lowest compressive strain that yielded a 0-value determinant of the global stiffness matrix corresponded to buckling.

The following general linear equation for the buckling perturbation of a thin plate with curvatures in the x and y directions caused by general loads is obtained by substituting Eq 2 into Eq 1

$$H_{11}\frac{\partial^4 w}{\partial x^4} + H_{22}\frac{\partial^4 w}{\partial y^4} + (2H_{12} + H_{33})\frac{\partial^4 w}{\partial x^2 \partial y^2} + 2H_{13}\frac{\partial^4 w}{\partial x^3 \partial y} + 2H_{23}\frac{\partial^4 w}{\partial x \partial y^3} - \frac{12}{h^3}\left(N_{11}\frac{\partial^2 w}{\partial x^2} + 2N_{12}\frac{\partial^2 w}{\partial x \partial y} + N_{22}\frac{\partial^2 w}{\partial y^2}\right) = 0 \qquad (3)$$

The solution technique applied to Eq 3 for CD buckling in Ref 2 was to reduce its form to a characteristic equation having four roots and to derive expressions for the K_{ij} in terms of the roots. This paper implements the same technique to analyze MD buckling, but first makes the general perturbation more specific.

The stress-strain relation proposed by Johnson and Urbanik *[6]* and used here to characterize the MD edgewise compression of paper is

$$\sigma(\epsilon_1) = d_1 \tanh(d_2\epsilon_1/d_1) \qquad (4)$$

where σ is stress, ϵ_1 is MD strain, and d_1 and d_2 are material constants (Fig. 2). Equation 4 is written for the MD of paper so that d, and d_2 are appropriate to that direction. The same form of relation with different material constants holds for uniaxial compression in any dkection. Constants d_1 and d_2 are used to distinguish them fmm constants c_1 and c_2 used for the CD.

Nonlinear Beam-Column Formulas

A subsection of corrugated fiberboard (Fig. 3) can be treated as a repeating sequence of linerboard microplates and core

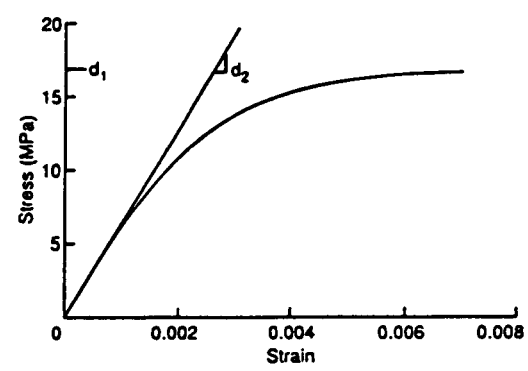

FIG. 2—*Optimum estimate of MD stress-strain curve of 204-g/m² linerboard examined in study and characterized by* d_1 = *16.8 MPa,* d_2 = *6.38 GPa, and* σ_c = *16.6 MPa.*

[2]All equations with decimal notation represent expressions from the referenced sources.

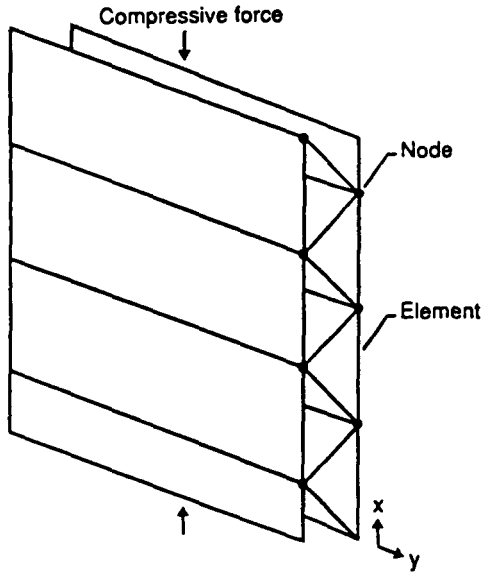

FIG. 3— *Structural section with flat plate elements. The x direction is aligned with the MD: the y direction is aligned with the CD.*

microplates subjected to compression and bending. When a section of corrugated fiberboard is compressed in the plane perpendicular to the corrugation axes, linerboard waviness in the *y* direction compared to waviness in the *x* direction is not observed to be significant. For honeycombs analyzed in Ref 4, good agreement between theory and experiments was obtained without considering cellular wall waviness transverse to the primary buckling curvature. Therefore, to characterize the deformation of each fiberboard microplate like the response of a short wide column, Eq 3 for buckling perturbation can be applied and curvature in they direction can be neglected. The following more specific buckling equation for MD compression is then obtained

$$H_{11}\frac{\partial^4 w}{\partial x^4} - \frac{12}{h^3}N_{11}\frac{\partial^2 w}{\partial x^2} = 0 \tag{5}$$

Equation 5 has the same form as the formula for a beam-column analysis for which solutions in the case of a linear material and various loading conditions are readily obtainable *[7]*.

For nonlinear paper, the bending stiffness H_{11} and force resultant N_{11} vary with strain. The theory of Johnson and Urbanik *[6]* predicts the H_{11} in the *x* direction varying with strain in the *x* direction to be

$$H_{11} = \frac{d_2}{\cosh^2(d_2\epsilon_1/d_1)} + \frac{\nu_1\nu_2 d_1}{1-\nu_1\nu_2}\frac{\tanh(d_2\epsilon_1/d_1)}{\epsilon_1} \tag{6}$$

where ν_1 and ν_2 are Poisson's ratios associated with *x*- and *y*-direction compressions, respectively. Neglecting y-direction waviness gives rise to a loading condition in which strain in the *y* direction is unrestrained. The load condition in the theory of Johnson and Urbanik *[6]* to consider in this paper for the prebuckled plate is then

$$N_{11} = -N_0 = -hd_1\tanh(d_2\epsilon_1/d_1) \tag{7}$$

where N_0 is the MD uniaxial compression load applied to the plate (Fig. 4).

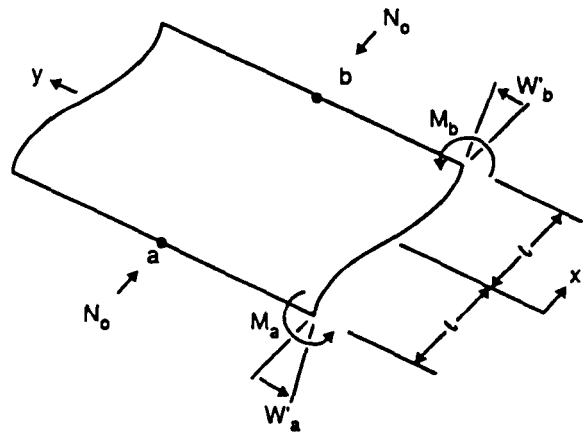

FIG. 4- *Sign convention for positive edge moments and positive slopes along element edge. In the equations taken from Ref 6, Subscript 1 relates to the y direction and Subscript 2 relates to the x direction.*

The general solution to Eq 5 is given by

$$w = a_1\sin\beta x + a_2\cos\beta x + a_3 x + a_4 \tag{8}$$

in which β is given by

$$\beta = \sqrt{\frac{12N_0}{h^3H_{11}}} \tag{9}$$

Constants a_1, a_2, a_3, and a_4 depend on plate boundary conditions.

Dimensionless Characterization

To obtain a dimensionless solution of Eq 5, the geometric mean Poisson's ratio

$$\nu = \sqrt{\nu_1\nu_2} \tag{10}$$

and the dimensionless variables

$$\hat{\beta} = \beta l, \qquad \hat{\epsilon} = \frac{d_2\epsilon_1}{d_1}, \qquad S = \frac{d_2}{d_1}\left(\frac{h}{2l}\right)^2 \tag{11}$$

are introduced, where 1 is the plate half-width in the *x* direction (Fig. 4) and *S* is a normalized plate stiffness. The centerline of the plate is chosen as $x = 0$ as consistent with the previous CD theory. Substituting Eqs 6 and 7 into Eq 9 and combining terms to obtain the expressions of Eqs 10 and 11 produce

$$\hat{\beta} = \left\{\frac{3\hat{\epsilon}}{S}\left[\frac{1}{1-\nu^2} - f(\hat{\epsilon})\right]^{-1}\right\}^{1/2} \tag{12}$$

where

$$f(\hat{\epsilon}) = 1 - \frac{2\hat{\epsilon}}{\sinh 2\hat{\epsilon}} \tag{13}$$

The solution to Eq 5 in terms of a normalized buckling strain is obtained by solving Eq 12 for $\hat{\epsilon}$

$$\hat{\epsilon} = \frac{\hat{\beta}^2 S}{3}\left[\frac{1}{1-\nu^2} - f(\hat{\epsilon})\right] \tag{14}$$

The value of $\hat{\beta}$ in Eq 14 must be determined from plate boundary conditions applied to Eq 8.

Solution for Buckling Stress

An understanding of column-like plate buckling when the edge conditions along $x = \pm 1$ (Fig. 4) are simple or fixed is useful for the case of elastic end conditions in a structure. With the centerline of the plate at $x = 0$, the boundary conditions for simple support are

$$x = \pm l : w = \frac{\partial^2 w}{\partial x^2} = 0 \tag{15}$$

Imposing these boundary conditions on Eq 8 leads to the formula $\sin \hat{\beta} \cos \hat{\beta} = 0$, from which $a_1 = a_3 = a_4 = 0$ and $\hat{\beta} = \pi/2$ for the lowest buckling mode. In terms of Eq 14, the critical buckling strain for simple support is solved from

$$\hat{\epsilon} = \frac{\pi^2 S}{12}\left[\frac{1}{1-\nu^2} - f(\hat{\epsilon})\right] \tag{16}$$

In Eq 16, the value of $\hat{\epsilon}$ was found to be solvable by Newton's iteration. An initial estimate of $\hat{\epsilon}$ is obtainable from the solution of the linearized theory for simple support:

$$\text{initial } \hat{\epsilon} = \frac{\pi^2 S}{12(1-\nu^2)} \tag{17}$$

For fixed edges, the boundary conditions are

$$x = \pm l : w = \frac{\partial w}{\partial x} = 0 \tag{18}$$

Imposing these conditions on Eq 8 yields $\sin \hat{\beta}(\hat{\beta} \cos \hat{\beta} - \sin \hat{\beta}) = 0$, from which $a_1 = a_3 = 0$, $a_2 = a_4$, and $\hat{\beta} = \pi$ for the lowest mode. The buckling strain with fixed edges is solved from

$$\hat{\epsilon} = \frac{\pi^2 S}{3}\left[\frac{1}{1-\nu^2} - f(\hat{\epsilon})\right] \tag{19}$$

An initial estimate of $\hat{\epsilon}$ for Newton's iteration needs to be obtained from the simple edge solution. Knowing $\hat{\epsilon}$, the buckling strain is $\epsilon_1 = d_2\hat{\epsilon}/d_1$ and the buckling stress by Eq 4 is $\sigma_b = \sigma(\epsilon_1)$. A normalized buckling stress from Eq 4 is given by

$$\hat{\sigma} = \frac{\sigma_b}{d_1} = \tanh \hat{\epsilon} \tag{20}$$

Normalized Buckling Stress and Strain Response

Results of the calculations for normalized buckling stress and normalized buckling strain are shown in Figs. 5 to 8. Figures 5 and 6 show how $\hat{\epsilon}$ and $\hat{\sigma}$, respectively, vary with stiffness S. Typical S values of the linerboard component in C-flute corrugated fiberboard (Fig. 1) can be 0.5 to 4 over the range of commercially available basis weights. Figure 7 shows how the ratio of fixed-edge $\hat{\sigma}$ to simple-edge $\hat{\sigma}$ varies with S. For MD-loaded corrugated fiberboard and a linerboard section of stiffness S, Fig. 7 predicts the maximum linerboard strength increase resulting from corrugated medium stiffness. As S approaches 0, the $\hat{\sigma}$ ratio approaches 4 and predicts the maximum strength increase to be expected. By comparison, Fig. 3 of Johnson and Urbanik *[1]* predicts that linerboard strength in CD-loaded fiberboard can be increased up to

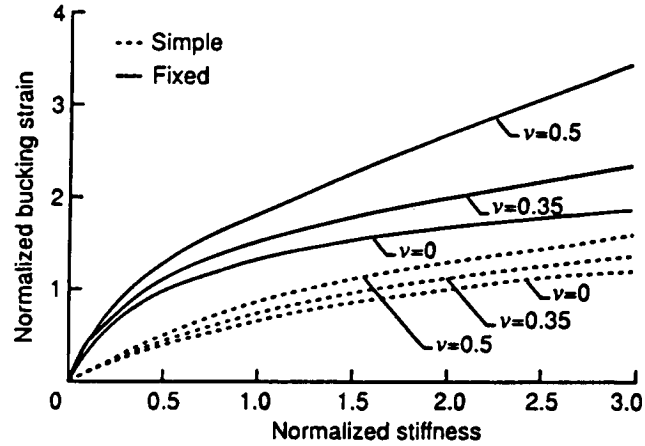

FIG. 5—*Plots of normalized buckling strain $\hat{\epsilon}$ as a function of normalized stiffness S for three mean Poisson's ratios and two edge-support conditions.*

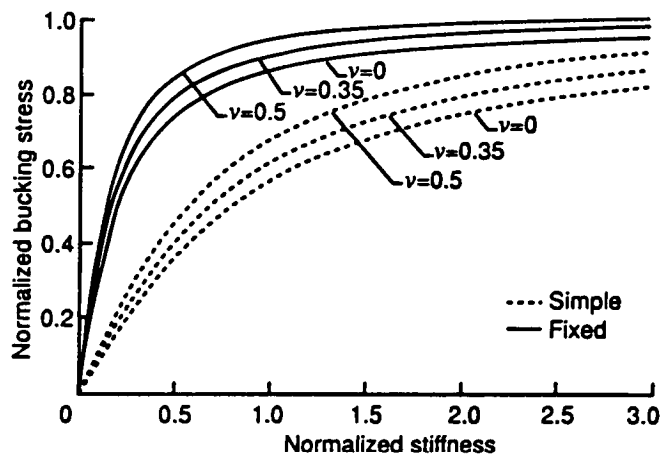

FIG. 6—*Plots of normalized buckling stress $\hat{\sigma}$ as a function of normalized stiffness S for three mean Poisson's ratios and two edge-support conditions.*

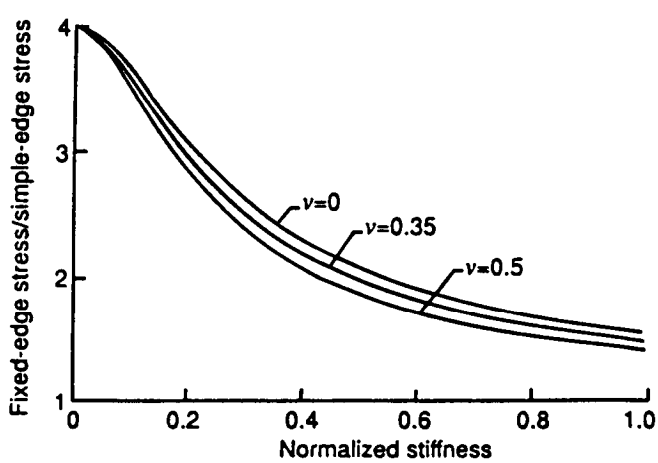

FIG. 7—*Ratios of fixed-edge buckling stress to simply-supported buckling stress as a function of normalized stiffness S for three mean Poisson's ratios.*

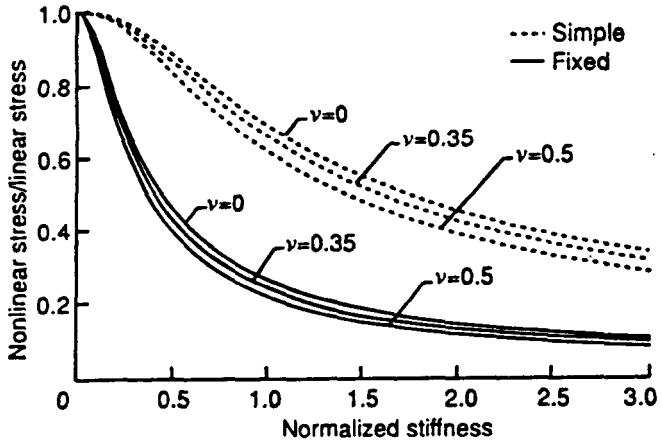

FIG. 8—*Ratios of nonlinear elastic buckling stress to linear elastic buckling stress as a function of normalized stiffness* S *for three mean Poisson's ratios and two edge-support conditions.*

1.75 times the simple support condition. Figure 8 shows the ratio of nonlinear $\hat{\sigma}$ to linear $\hat{\sigma}$ varying with S and quantifies the importance of applying a nonlinear characterization of material.

MD Buckling of Corrugated Fiberboard

Moment-Curvature Relationships

Structure buckling strength (Fig. 3) can be determined in accordance with the finite element technique of Johnson and Urbanik *[2]* if an element stiffness matrix for each linerboard element and core element is first constructed from respective stress-strain properties. For a corrugated structure subjected to MD compression, it is now assumed that common edges along linerboard-medium attachment points remain straight, and that edge rotation is a function of the attached element stiffnesses.

Establish local labels a and b at the edges $x = -l$ and $x = l$, respectively, of the plate (Fig. 4). Define the edge rotations w'_a and w'_b at nodes a and b to be

$$w'_a = \left.\frac{\partial w}{\partial x}\right|_{-l} \qquad w'_b = \left.\frac{\partial w}{\partial x}\right|_{l} \tag{21}$$

Taking the moment resultant M_{11} given by Eq 2 and neglecting curvature in the y direction along an edge lead to

$$x = \pm l : M_{11} = -\frac{1}{12} h^3 H_{11} \frac{\partial^2 w}{\partial x^2} \tag{22}$$

Define the edge moments M_a and M_b corresponding to w'_a and w'_b respectively, to be

$$M_a = M_{11}|_{-l} \qquad M_b = -M_{11}|_{l} \tag{23}$$

Equations 21 and 23 use the sign convention that edge rotations and edge moments are positive when directed counterclockwise (Fig. 4).

The boundary conditions for elastic edges are

$$x = -l : w = 0; \quad \frac{\partial w}{\partial x} = w'_a \quad x = l : w = 0; \quad \frac{\partial w}{\partial x} = w'_b \tag{24}$$

Substituting derivatives of Eq 8 into Eq 24 and solving the four boundary condition equations yield

$$\begin{aligned} a_1 &= \frac{(w'_a + w'_b)l}{2(\hat{\beta}\cos\hat{\beta} - \sin\hat{\beta})}, \\ a_2 &= \frac{(w'_a - w'_b)l}{2\hat{\beta}\sin\hat{\beta}}, \\ a_3 &= -\frac{a_1 \sin\hat{\beta}}{l}, \\ a_4 &= -a_2\cos\hat{\beta} \end{aligned} \tag{25}$$

Element Stiffness Matrix

Edge moments and edge rotations are related by the matrix formula

$$\begin{bmatrix} M_a \\ M_b \end{bmatrix} = \begin{bmatrix} K_{aa} & K_{ab} \\ K_{ba} & K_{bb} \end{bmatrix} \begin{bmatrix} w'_a \\ w'_b \end{bmatrix} \tag{26}$$

With the substitution of the a_1 to a_4 values from Eq 25 into the derivative expressions in Eqs 21 to 23, a solution to the stiffness matrix of Eq 26 is given by

$$\begin{bmatrix} K_{aa} & K_{ab} \\ K_{ba} & K_{bb} \end{bmatrix} = \frac{1}{24}\frac{h^3 H_{11}}{l}\hat{\beta}^2 \begin{bmatrix} k_1 + k_2 & k_1 - k_2 \\ k_1 - k_2 & k_1 + k_2 \end{bmatrix} \tag{27}$$

where

$$k_1 = \frac{\tan\hat{\beta}}{\tan\hat{\beta} - \hat{\beta}} \qquad k_2 = \frac{1}{\hat{\beta}\tan\hat{\beta}} \tag{28}$$

The stiffness coefficients by Eq 27 are appropriate for the linerboard components subjected to MD strain during MD fiberboard compression. When $\epsilon_1 = 0$, Eq 27 is reduced to the linear elastic form given by

$$\begin{bmatrix} K_{aa} & K_{ab} \\ K_{ba} & K_{bb} \end{bmatrix} = \frac{1}{24}\frac{h^3 d_2}{l(1 - \nu^2)} \begin{bmatrix} 4 & 2 \\ 2 & 4 \end{bmatrix} \tag{29}$$

Therefore, for the corrugated medium components subjected only to bending, stiffness coefficients by Eq 29 are appropriate.

Global Stiffness Matrix

With element stiffness matricies given by Eqs 27 and 29 for the fiberboard components in terms of local node labels, a global stiffness matrix for the structure needs to be constructed. The same technique for element counting and node labeling given by Johnson and Urbanik *[2]* is applied. The result is a global stiffness matrix [SK]. Elements of matrix [SK] are functions of the axial strain ϵ_1 applied to the structure. The critical strains are those values for which matrix [SK] is singular. These critical strains are hence solutions of the equation

$$F(\epsilon_1) \equiv \det[\mathbf{SK}] = 0 \tag{30}$$

The same algorithm used by Johnson and Urbanik [2] also yielded a solution to Eq 30. From the lowest critical strain, the structure buckling load is given by $P_b = \Sigma N_0$ in which art N_0 level corresponding to each linerboard component is determined from Eq 7 and respective stress-strain properties.

Results

Previous Data

Data taken from an independent compression strength study *[8]* provide a test of the MD ECT theory given here. In a subset of the data reported there, six nominal basis weight (BW) levels of fourdrinier kraft linerboard supplied by one paper mill and five nominal BW levels of semichemical corrugating medium supplied by three mills were combined to yield 30 combinations of corrugated fiberboard. (Currently, almost all linerboard is produced by the fourdrinier process.) Corrugating was performed on a C-flute production corrugator with 128 flutes/m (39 flutes/ft).

Among the data reported linerboard materials were tested for a unit-width MD compression strength S_u, MD extensional stiffness EA_u, and MD flexural stiffness EI_u. Here E is the initial modulus of elasticity of the material; A_u and I_u represent an effective cross-sectional area and an effective moment of inertia respectively, per width of material. Corrugating medium materials were tested for surface-to-surface thickness t and CD EA_u. Average values of linerboard data and medium data at each BW level are given in Tables 1 and 2, respectively.

Short columns of the corrugated fiberboard were tested for MD ECT strength. Strength data are summarized in Table 3. The first number in each cell of the table is the average experimental ECT strength P. The second number in parentheses is a predicted failure load P_f based on a column design formula to be presented later.

TABLE 1—*Average MD properties of linerboard.*

	Measurement			Property		
BW, g/m²	S_u, kN/m	EA_u, MN/m	EI_u, mN · m	σ_c, MPa	d_2, GPa	h, μm
139	3.17	1.14	3.93	15.6	5.61	203
169	3.93	1.39	6.02	17.2	6.10	228
207	4.62	1.78	11.5	16.6	6.38	278
278	5.32	2.29	27.8	13.9	5.99	382
333	6.00	2.35	39.4	13.4	5.23	449
437	7.84	3.03	82.2	13.7	5.31	571

TABLE 2—*Average CD properties of corrugating medium.*

	Measurement		
BW, g/m²	t, mm	EA_u, kN/m	c_2, GPa
85	153	315	2.06
136	253	389	1.54
165	308	545	1.77
189	378	602	1.59
270	422	883	2.09

Stress-Strain Approximations

For inputs to determining the linerboard stiffness coefficients by Eq 27, the paper data in Table 1 were converted to stress-strain properties, and approximations were applied wherever data were incomplete. The average linerboard stress-strain properties of h, ultimate crush stress σ_c, and d_2 are given in Table 1. Material thickness h is an effective thickness given by the formula

$$h = \sqrt{12 \frac{EI_u}{EA_u}} \tag{31}$$

Having h, properties σ_c and d_2 were calculated from $\sigma_c = S/h$ and $d_2 = EA/h$. Since an exact value of d_1 could not be determined from data, the initial approximation by $d_1 \sim \theta_0\sigma_c$ using $\theta_0 = 1$ was assumed (Fig. 2). Corrugating medium values of h and d_2 for calculating stiffness coefficients by Eq 29 were not obtainable from [8]. Therefore, initial approximations by $h \sim t$ and $d_2 \sim \theta_3 c_2$ using $\theta_3 = 1$ were used. The geometric mean Poisson's ratio $\nu = 0.268$ used in previous research *[6]* was also used here to characterize the linerboard and rnedium materials.

Material Crush Strength

Short-column strength of corrugated fiberboard was first compared with the material crush strength P_c equal to the sum of strengths $2S_u$ of the linerboard components. As expected, adding the linerboard compression stengths was a poor predictor of short-column MD ECT strength. Figure 9 shows how the prediction errors between P_c and P varied with linerboard BW level. The errors are plotted as a percentage of P. The crush failure predictions ranged from an average of 134% too high for the lowest B W linerboard to an average of 10% too high for the highest BW linerboard. It can be inferred from Figs. 6 and 9 that ECT failure with low BW linerboards resulted from buckling. The variation of crush failure predictions with corrugating medium BW level are plotted in Fig. 10. Average predictions ranged from 74% too high for the lowest BW medium to 27% too high for the highest BW medium. The trend shown Fig. 10) has a weak statistical significance, but it is consistent with the theoretical effect of the corrugating medium stiffness on the local buckling of the linerboard.

Short-Column Buckling Load

Short-column strength was compared with the buckling load P_b equal to the sum of loads $2N_0$ on the linerboard components at the lowest critical strain. Here N_0 was calculated from Eq 7 after the critical strain ϵ_1 was determined by Eq 30. In addition to the stress-strain properties given previously, and based on typical C-flute corrugating geometry, dimension $2l$ (Fig. 4) characterizing the paperboard length between flute attachment points was taken to be $2l$ = 7.82 mm for the linerboard and $2l$ = 5.67 mm for the corrugated medium. Single-face and double-back components of combined board were considered as equal, and the effects of corrugating stress and adhesive on geometry were ignored.

These initial estimates of stress-strain properties and geometry yielded art average error between P_b and P of only 8.0% (r^2 = 0.979). Nevertheless, the prediction errors still varied with linerboard BW (Fig. 11). For the stress-strain inputs used, buckling theory was most accurate for low BW materials, but was too

TABLE 3—*MD ECT strength of corrugated fiberboard compared with predicted strength.*

Corrugated Medium BW, g/m²	Actual and Predicted (in parentheses) Strength, kN/m, at Various Linerboard BW					
	139 g/m²	169 g/m²	207 g/m²	278 g/m²	333 g/m²	437 g/m²
85	1.68 (1.97)	2.45 (2.68)	4.27 (4.12)	6.97 (6.70)	8.58 (8.08)	11.8 (11.9)
136	2.56 (2.47)	3.43 (3.52)	5.52 (5.45)	7.81 (8.20)	10.4 (9.69)	12.8 (13.6)
165	2.68 (2.59)	3.61 (3.74)	5.29 (5.78)	8.62 (8.57)	9.61 (10.1)	14.4 (14.1)
189	2.94 (2.64)	3.78 (3.82)	5.29 (5.89)	9.25 (8.69)	10.6 (10.3)	13.7 (14.3)
270	3.05 (2.67)	4.12 (3.87)	5.50 (5.97)	8.86 (8.77)	10.8 (10.3)	14.9 (14.4)

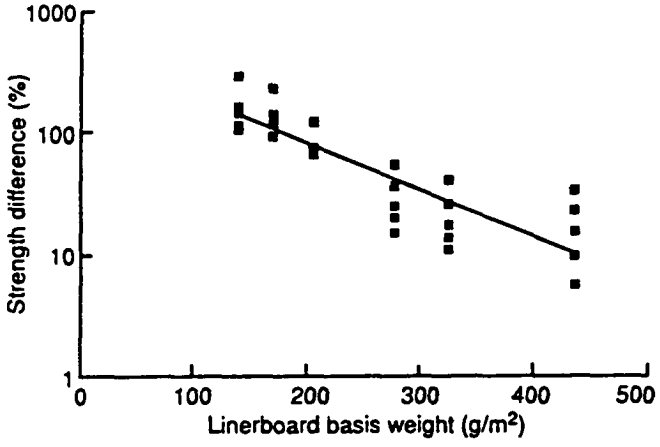

FIG. 9—*Strength difference between sum of linerboard MD compression strength and corrugated fiberboard MD compression strength as a function of linerboard basis weight. Points represent prediction level above data. The line is an exponential regression fit to data;* $r^2 = 0.758$.

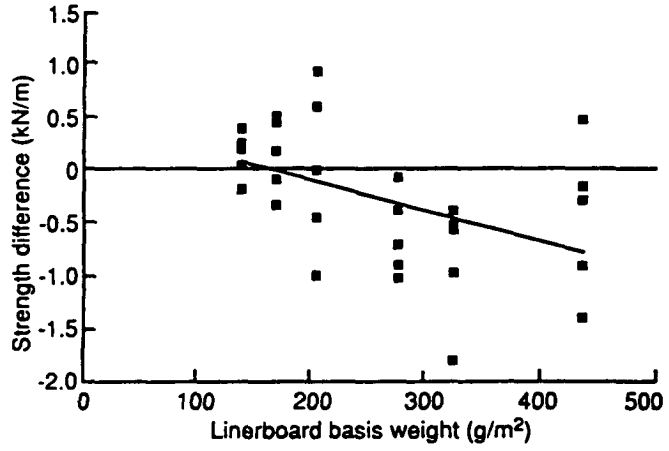

FIG. 11—*Strength difference between sum of linerboard MD buckling loads and corrugated fiberboard MD compression strength as a function of linerboard basis weight. Points represent prediction level above data. The line a regression fit to data;* $r^2 = 0.231$.

conservative for high BW materials. Predictions were found to be empirically improvable if short-column failures are considered to result from combined crushing and buckling and if values of θ_0 and θ_3 are optimized to reflect property input errors.

Crushing and Buckling Interaction

In the design of wood columns failure was considered to be a mixed-mode interaction between material crushing and column buckling *[5]*. For linear materials, researchers have proposed various column design formulas to characterize a mixed-mode progression from buckling to crushing as universal slenderness decreases. Universal slenderness $U = \sqrt{P/P_b}$, the square root of the ratio between crushing strength and buckling strength. For application to a material with a nonlinear stress-strain curve according to Eq 4 and an effective thickness that remains constant, U conveniently reduces to a function of&. An expression for U is given by

$$U^2 = \frac{\sigma_c}{\sigma_b} = \frac{\sigma_c}{d_1\hat{\sigma}} = \frac{\sigma_c}{\theta_0\sigma_c\hat{\sigma}} = \frac{1}{\theta_0\hat{\sigma}} \tag{32}$$

in which θ_0 expresses the ratio d_1/σ_c.

For the previous P and P_c data of this study, the variation of the crushing interaction P/P_c with slenderness U is plotted in Fig. 12. The interaction between crushing and buckling is observable by superimposing a plot of the buckling interaction P_b/P_c varying with U (Fig. 12). Unlike the design formulas advocated by Zahn *[5]* to correct for increasing errors between P and P_c as U decreases for linear materials, a simpler design formula can be inferred from Fig. 12 for nonlinear corrugated fiberboard.

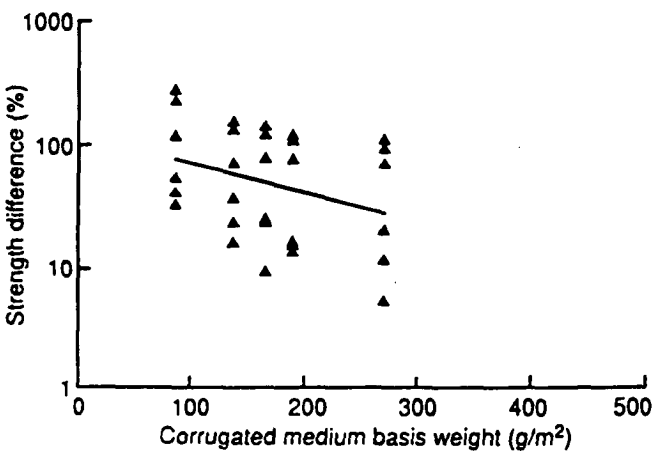

FIG. 10—*Strength difference between sum of linerboard MD compression strength and corrugated fiberboard MD compression strength as a function of corrugated medium basis weight. Points represent prediction level above data. The line is an exponential regression fit to data;* $r^2 = 0.110$.

Design Formula

Consider a material failure stress σ_f corresponding to structure failure at load P_f. In Fig. 12, the crushing interaction in terms of stress varies empirically with universal slenderness according to

$$\log\left(\frac{\sigma_f}{\sigma_c}\right) = \alpha \log\sqrt{\frac{1}{\theta_0\hat{\sigma}}} \tag{33}$$

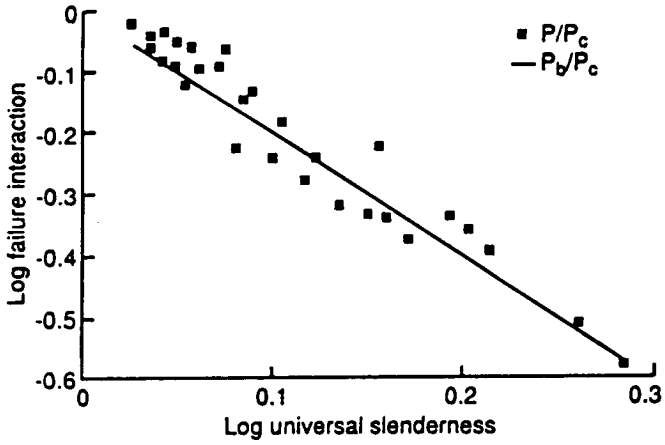

FIG. 12—*Comparison between material crush interaction plotted as the ratio* P/P_c *and buckling interaction plotted as the ratio* P_b/P_c *varying with universal slenderness given by* $\sqrt{P_c/P_b}$.

from which

$$\sigma_f = \sigma_c \theta_0^{\theta_2} \hat{\sigma}(\theta_0)^{\theta_2} \tag{34}$$

where $\theta_2 = -\alpha/2$ and $\hat{\sigma}$ is written as a function of θ_0 to express the fact that the value of d_i input to detetining Sand thus $\hat{\sigma}$ (Fig. 6) has been made dependent upon θ_0. From the above stress formula element load-carrying ability is predicted to be $N_f = h\sigma_f$; structure failure load becomes $P_f = \Sigma N_f$.

An optimum fit of P_f to P data yielded an average error of 5.4% (r^2 = 0.990) (Fig. 13) and was obtained with θ_0 = 1.01 ± 0.0097, θ_2 = 1.59 ± 0.092, and θ_3 = 8.79 ± 1.7 in Eq 34; the ± numbers, represent 95% confidence intervals. Predicted ECT strength values are given in parentheses in Table 3. The value of θ_0 = 1.01 reflects the experimental errors in quantifying the stress-strain relationship and stiffness S by Eq 11 and compares with c_1/σ_u = 1.33 reported by Urbanik *[9]* for CD paper tests. The value θ_2 = 1.59 yields more conservative buckling strength predictions for low BW linerboards. The value θ_3 = 8.79 is a function of experimental errors and the material property estimations in determining the stiffness coefficients by Eq 29. After allowing for $d_2/c_2 \approx 2.0$, the optimum θ_3 value seems high. Additional tests should be made with complete material characterizations.

The variation of linerboard $\hat{\sigma}$ with S predicted by the Eq 34 optimization is plotted in Fig. 14. From the separation of data by BW level, the results predict that the 270-.g/m^2 corrugated medium yielded a near fixed-edge condition for the linerboard. The 85-g/m^2 medium performed between simple and fixed conditions. The variation of the previous crush interaction with U is plotted again in Fig. 15. The variation of the improved buckling interaction with U, using optimum stress-strain properties to calculate P_b, is superimposed.

Conclusions

Linerboard elements between the Linerboard-medium attachment points of corrugated fiberboard can be viewed as short wide columns when the fiberboard is loaded in the machine direction. Colum ends are elastically restrained by the corrugated medium. A theory of machine-direction buckling of nonlinear corrugated fiberboard material, consistent with previous theory applied to fiberboard under cross-direction compression, was developed.

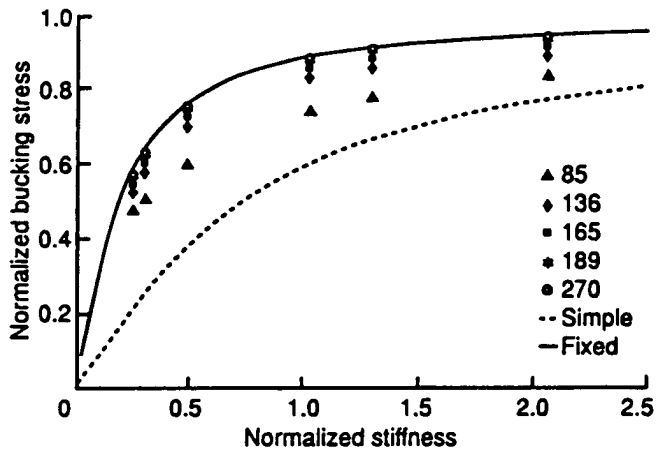

FIG. 14—*Plots of normalized buckling stress* $\hat{\sigma}$ *as a function of normalized stiffness* S *for Poisson's ratio* ν = 0.268 *and various edge-support conditions. The points represent linerboard supported by five basis weight levels (g/m*^{2}*) of corrugated medium. The lines are theoretical conditions.*

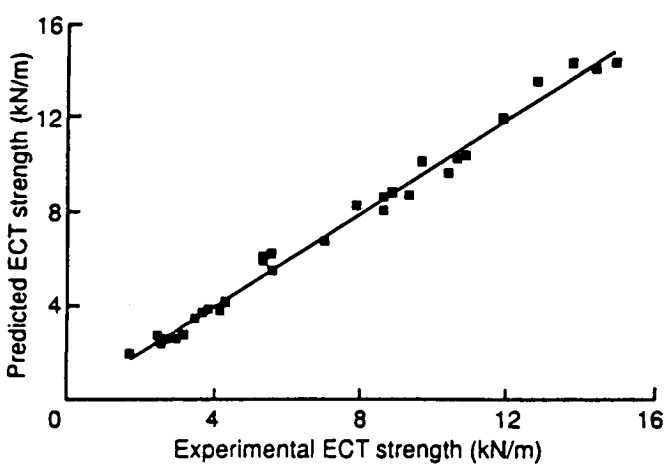

FIG. 13—*Comparison between predicted MD ECT strength* P_f *and experimental strength* P. *Points represent data; the line is a plot of equality; average error* = 5.4%; r^2 = 0.990.

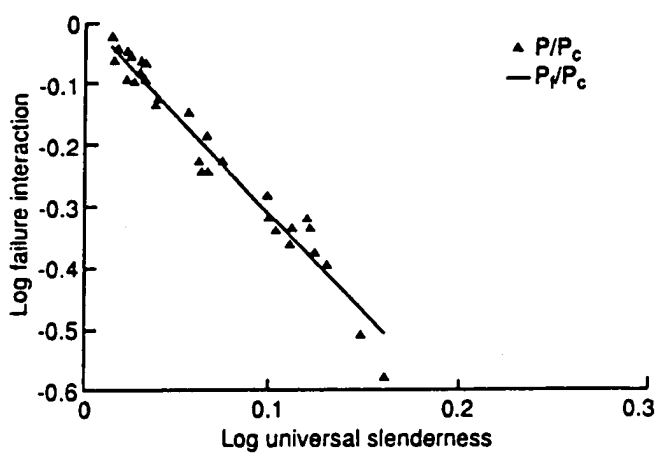

FIG. 15—*Comparison between material crush interaction plotted as the ratio* P/P_c *and crush-buckling interaction plotted as the ratio* P_f/P_c *varying with universal slenderness given by* $\sqrt{P_c/P_b}$.

Compared to strength data the theory had an average error of 8.0% using paper compression strength, extensional stiffness, and bending stiffness data as inputs. The theory was further improved and the average error was reduced to 5.4% by empirically correcting for interactions between material crush failure and structure buckling failure. The correction equation predicts an optimum form of the linerboard stress-strain curve from initial slope and maximum stress data and predicts art element slenderness that varies with the failure mode. Additional tests with complete material characterizations are needed to verify the affect of material approximations on ECT strength predictions and to verify the strain response predicted by the theory.

References

[1] Johnson, M. W., Jr. and Urbanik, T. J., "Buckling of Axially Loaded Long Rectangular Paperboard Plates," *Wood and Fiber Science*, Vol. 19, No. 2, April 1987, pp. 135–146.

[2] Johnson, M. W., Jr. and Urbanik, T. J., "Analysis of the Localized Buckling in Composite Plate Structures With Application to Determining the Strength of Corrugated Fiberboard," *Journal of Composites Technology & Research*, JCTRER, Vol. 11, No. 4, Winter 1989, pp. 121–127.

[3] Pommier, J. C., "The Linerboard Compression Factor," FEFCO, 7th Technical Seminar, Nice, France, April 1993.

[4] Gibson, L. J. and Ashby, M. F., *Cellular Solids*, Pergamon Press, 1988.

[5] Zahn, T. J., "Re-examination of Ylinen and other Column Equations," *Journal of Structural Engineering*, ASCE, Vol. 118, No. 10, October 1992, pp. 2716–2728.

[6] Johnson, M. W., Jr. and Urbanik, T. J., "A Nonlinear Theory for Elastic Plates With Application to Characterizing Paper Properties," *Journal of Applied Mechanics*, Vol. 51, March 1984, pp. 146–152.

[7] Timoshenko, S. P. and Gere, J. M., *Theory of Elastic Stability*, McGraw-Hill, 1961.

[8] The Institute of Paper Chemistry, "The Effect of Distribution of Stiffness Between Components on the Compression Performance of Corrugated Boxes," Testing, Compression 85, Project 2695-3, 1967, pp. 1–52.

[9] Urbanik, T. J., "Correcting for Instrumentation With Corrugated Fiberboard Edgewise Crush Test Theory," *Tappi Journal*, Oct. 1990, pp. 263–268.